

EPR and magnetic susceptibility studies of iron ions in $3\text{B}_2\text{O}_3\cdot\text{SrO}$ glass matrix

I. ARDELEAN, R. LUNGU, P. PASCUTA^a

Faculty of Physics, Babes-Bolyai University, 400084 Cluj-Napoca, Romania

^aDepartment of Physics, Technical University, 400641 Cluj-Napoca, Romania

EPR and magnetic susceptibility measurements have been performed on $x\text{Fe}_2\text{O}_3\cdot(100-x)$ [$3\text{B}_2\text{O}_3\cdot\text{SrO}$] glasses, with $0 \leq x \leq 40$ mol%. When increasing the iron content the EPR absorption spectra undergo modification reflecting structural changes of the glass matrix and also the distribution and valence states of iron ions. The magnetic measurement data pointed out the valence state and the character of interaction involving iron ions as depending on concentration and the simultaneous presence of both Fe^{3+} and Fe^{2+} ionic species.

(Received May 15, 2008; accepted June 4, 2008)

Keywords: $\text{B}_2\text{O}_3\cdot\text{SrO}$, ESR, Susceptibility, Glass

1. Introduction

Glasses containing transition metal ions (TMI) were the subject of a great deal of interest in the past three decades due to their important technological applications in electronics, tunable solid state lasers and optical telecommunication [1-3]. On the other hand TMI, e.g. iron, are often used as probes in exploring the structure of new vitreous systems, by means of their electron paramagnetic resonance (EPR) absorption spectra [4-18]. The valence states of iron ions involved in many glass systems reported up to date are Fe^{3+} and Fe^{2+} , but only Fe^{3+} (3d^5 , $^6\text{S}_{5/2}$) shows EPR absorptions at room temperature [4-18]. EPR of Fe^{3+} ions may provide useful information concerning the structural details of the vitreous matrix revealed by their distribution on different structural units building the network, their coordination and the valence state. It is also possible to follow the local changes in the glass matrix when iron ions concentration increases during a controlled doping process. Data were reported for a great variety of glasses as borate [5,7,11,14,16,18], phosphate [8,12], bismuthate [13,17], tellurite [9,10], silicate [4, 15] and germanate [6], where Fe^{3+} species were detected as isolated in strongly distorted vicinities, options for the rhombic or tetragonal symmetries subjected to strong ligand field effects and interacting by dipolar or superexchange coupled pairs, depending on the Fe_2O_3 content in glasses.

Useful information about the valence states and interactions involving iron ions in glasses were obtained by means of magnetic measurements. The superexchange interaction of the iron ions in the oxide glasses was most frequently attributed to an antiferromagnetic coupling within the pairs $\text{Fe}^{3+}\text{-Fe}^{3+}$, $\text{Fe}^{3+}\text{-Fe}^{2+}$ and $\text{Fe}^{2+}\text{-Fe}^{2+}$ [9, 19]. An antiferromagnetic coupling between iron ions was reported in borate [8,20], phosphate [21,22], tellurite [9,10], bismuthate [23], silicate [24] and germanate [25]

oxide glasses. The antiferromagnetic behaviour depends on the concentration range of iron, the glass matrix structure [26], the preparation conditions [27] and consequently on the $\text{Fe}^{3+}/\text{Fe}^{2+}$ ratio [28].

This work aims to present our results obtained by means of EPR and magnetic susceptibility measurements performed on $x\text{Fe}_2\text{O}_3\cdot(100-x)$ [$3\text{B}_2\text{O}_3\cdot\text{SrO}$] glasses revealed by distribution of iron ions in various structural formation, their valence states and magnetic interactions involving them. The research is part of a comparative analysis program focused on the behaviour of TMI in vitreous oxide matrices.

2. Experimental procedure

We have prepared $x\text{Fe}_2\text{O}_3\cdot(100-x)$ [$3\text{B}_2\text{O}_3\cdot\text{SrO}$] glasses using pure reagent grade Fe_2O_3 , H_3BO_3 and SrCO_3 . The samples were prepared by weighing suitable proportions of components, powder mixing and mixture melting in sintered corundum crucibles at 1200 °C for 30 minutes. The mixtures were put into the furnace direct at this temperature. The melts were poured onto stainless steel plates.

The X-Ray diffraction measurements were made with a Philips X'Pert MPD diffractometer, with a monochromator of graphite for $\text{CuK}\alpha$ ($\lambda=1.540560$ Å). The pattern obtained did not reveal any crystalline phase in the samples up to 40 mol % Fe_2O_3 .

The EPR measurements were made using a Portable Adani PS 8400 spectrometer in X-band (9.1-9.6 GHz) and 100 kHz field modulation. The measurements were made at room temperature. To avoid the alteration of the glass structure due to the ambient conditions, especially humidity, samples were poured immediately after preparation and enclosed in tubular holders of the same caliber. Equal quantities of samples were studied.

The magnetic susceptibility measurements were made using a Faraday type magnetic balance in 80-300 K temperature range. Correction due to the diamagnetism of the Fe_2O_3 , B_2O_3 and SrO were taken into account in order to obtain the real magnetic susceptibility of iron ions in the studied glasses.

3. Results and discussion

The EPR absorption spectra were obtained for the $x\text{Fe}_2\text{O}_3\text{-}(100-x)[3\text{B}_2\text{O}_3\text{-SrO}]$ glasses with $0.5 \leq x \leq 40$ mol%. The main lines from the EPR spectra of iron doped samples (Fig. 1) are characterized by $g_{\text{eff}} \approx 4.3$ and $g_{\text{eff}} \approx 2.0$. The resonance line at $g_{\text{eff}} \approx 4.3$ is due to Fe^{3+} ions which are isolated and situated in sites of distorted octahedral symmetry (rhombic or tetragonal) subjected to strong crystal field effects [7,9,11,13]. The $g_{\text{eff}} \approx 2.0$ line may be attributed either to Fe^{3+} species interacting by dipole-dipole interaction in sites of less distorted octahedral (tetrahedral) field or to their superexchange coupled pairs [9,15,20]. The EPR spectra structure shows a strong dependence on the Fe_2O_3 content. The evolution of the resonance lines with increasing of iron ions content was followed in the dependence of the EPR parameters, i.e. the line intensity I , estimated as the line integral and the peak-to-peak linewidth ΔB . The corresponding variations of these parameters are plotted in Figs. 2 and 3 for the resonance lines at $g_{\text{eff}} \approx 4.3$ and $g_{\text{eff}} \approx 2.0$, respectively.

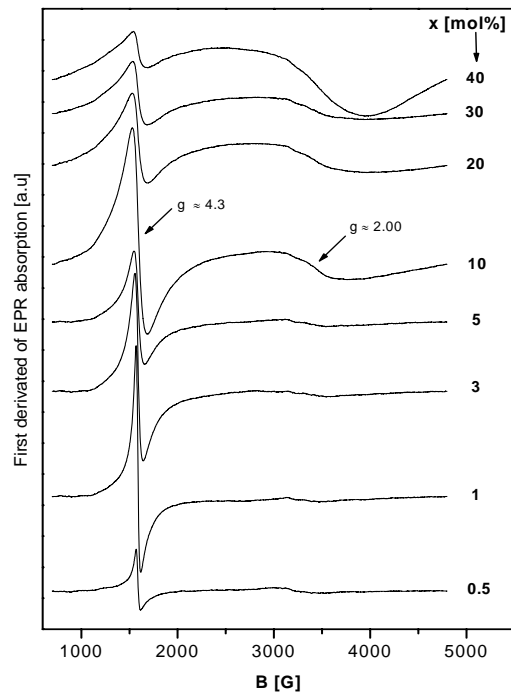
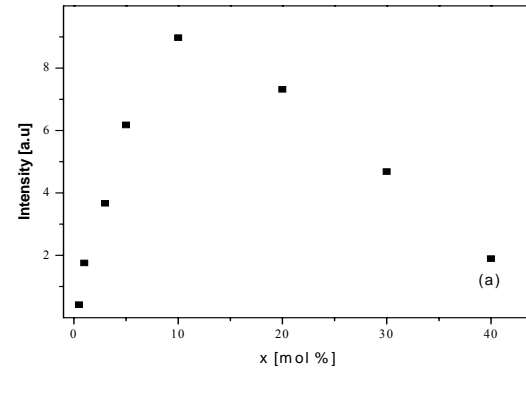
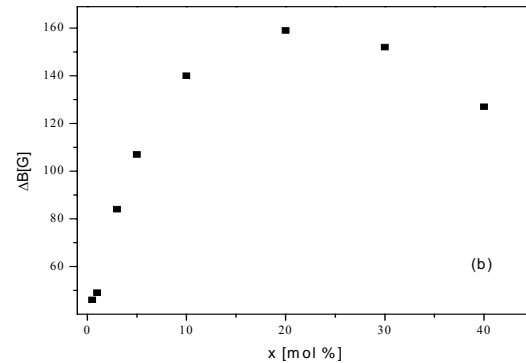


Fig. 1. EPR absorption spectra of Fe^{3+} ions in $x\text{Fe}_2\text{O}_3\text{-}(100-x)[3\text{B}_2\text{O}_3\text{-SrO}]$ glasses.

According to Fig. 2a the intensity of the absorption line centered at $g_{\text{eff}} \approx 4.3$ increases up to $x = 10$ mol% and after that strongly decreases. The decreasing of this resonance line intensity at the same time with the increasing of the Fe_2O_3 content is due to the destruction of the configuration from the iron ions vicinities, which assures their magnetic isolation. Although randomly distorted these vicinities are similar to each other having at the origin the same crystalline structure of oxides involved in preparing the vitreous matrix, and the same ability of Fe^{3+} in ordering the surrounding. These structural units assure the independence of the involved Fe^{3+} ions and their specificity of "isolated" ones. The gradual increasing of the iron content in the glass matrix destroys the local ordering of the Fe^{3+} ion vicinities, so the structural units as characteristic entities become less represented. Consequently the $g_{\text{eff}} \approx 4.3$ line intensity decreases. The linewidth evolution of the $g_{\text{eff}} \approx 4.3$ line (Fig. 2b) shows an increasing up to $x = 20$ mol%. For higher content of Fe_2O_3 , the linewidth decreases. According to the line intensity decreasing evidenced for $x > 10$ mol% (Fig. 2a), the decreasing of ΔB is due to the progressive decrease of the concentration of Fe^{3+} ions in structural vicinities giving rise to the $g_{\text{eff}} \approx 4.3$ absorption.



a



b

Fig. 2. Composition dependences of the line-intensity (a) and line-width (b) of resonance absorptions at $g \approx 4.3$.

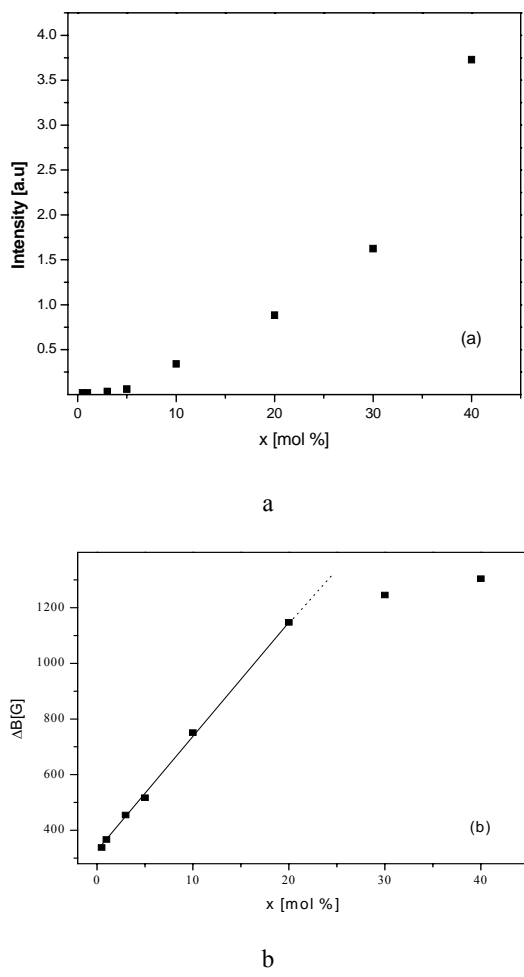


Fig. 3. Composition dependences of the line-intensity (a) and line-width (b) of resonance absorptions at $g \approx 2.0$.

The intensity of the resonance absorption line from $g_{\text{eff}} \approx 2.0$ increases in all whole concentration range, more evidenced for $x > 10 \text{ mol\%}$ (Fig. 3a). On the other hand, the line intensity of the absorptions from $g_{\text{eff}} \approx 4.3$ decreases for $x > 10 \text{ mol\%}$ (Fig. 2a), in consequence, at higher content of Fe_2O_3 ($x > 10 \text{ mol\%}$), the Fe^{3+} ions participated at dipole-dipole and/ or superexchange interactions. The linewidth of the $g_{\text{eff}} \approx 2.0$ line depends also on the Fe_2O_3 concentration (Fig. 3b) revealing the clustering capacity of the iron ions in the investigated matrix. The $\Delta B = f(x)$ dependence reflects the competition between the broadening mechanisms as the dipol-dipol interactions, the increased disordering of the matrix structure, the interactions between ions in different states and the narrowing ones that are the superexchange interactions within the pairs of iron ions. These mechanisms can act simultaneously but they are predominant in function of the Fe_2O_3 sample content. Following the $\Delta B = f(x)$ dependence it was observed a deviation from linearity of ΔB for $x > 20 \text{ mol\%}$. This suggests that for $x > 20 \text{ mol\%}$ can appear superexchange

interactions which narrow the resonance line from $g_{\text{eff}} \approx 2.0$. More intuitively, when the network sites available for the isolated impurities are occupied, the following iron ions enter the glass matrix in the position which determines a new structural ordering in the Fe^{3+} ion vicinities. Consequently, the glass structure became more complicated at higher Fe_2O_3 concentrations, which is then favorable to cluster formation of iron ions, coupled by superexchange interactions.

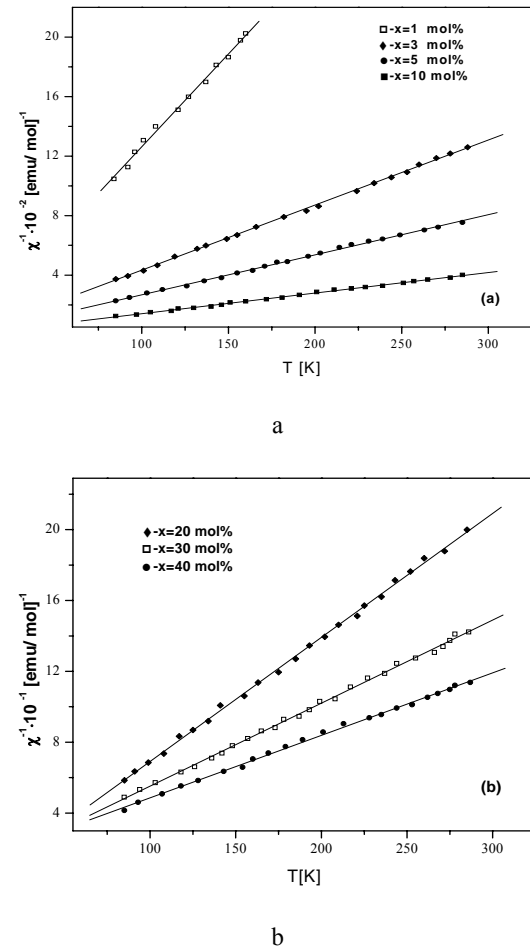


Fig. 4. Temperature dependence of the reciprocal magnetic susceptibility for $x\text{Fe}_2\text{O}_3 \cdot (100-x) [3\text{B}_2\text{O}_3 \cdot \text{SrO}]$ glasses with $1 \leq x \leq 10 \text{ mol\%}$ (a) and with $20 \leq x \leq 40 \text{ mol\%}$ (b).

The magnetic susceptibility data correlate well with the EPR result and also complete them. The temperature dependence of the reciprocal magnetic susceptibility (Fig. 4) shows for samples with $x \leq 20 \text{ mol\%}$ a paramagnetic behaviour of Curie type, suggesting that in this concentration range iron ions are predominantly isolated or/ and subjected to dipole-dipole interactions. For $x > 20 \text{ mol\%}$ the reciprocal magnetic susceptibility obeys a Curie-Weiss behavior with a negative paramagnetic Curie temperature (θ_p), characteristic to antiferromagnetic

coupling of magnetic ions. The peculiar structure specific to vitreous oxide solids impose the short-range character of magnetic interactions and enhance the structural image of clusters. The result agrees with data explaining the $g_{\text{eff}} \approx 2.0$ line narrowing as result of superexchange interactions between iron ions involved in cluster structure.

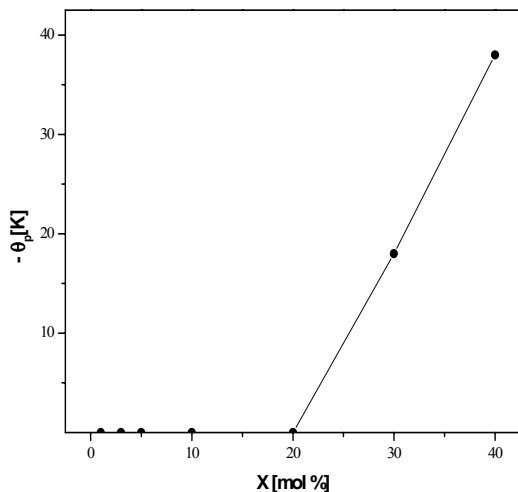


Fig. 5. Composition dependence of the paramagnetic Curie temperature.

The composition dependence of θ_p is given in Fig. 5. The absolute magnitude of θ_p values increases for $x > 20$ mol %. The exchange integral increase as the content of the magnetic ions is increased in the glass and as a result the absolute magnitude of the θ_p increases [19].

Table 1. Molar Curie constant and molar fraction of $\text{Fe}^{3+}(x_1)$ and $\text{Fe}^{2+}(x_2)$ ions in $x\text{Fe}_2\text{O}_3\text{-}(100-x)[3\text{B}_2\text{O}_3\text{-SrO}]$ glasses.

x [mol %] Fe_2O_3	$C_M \cdot 10^2$ [emu/mol]	x_1 [mol %] $\text{Fe}_2^{3+}\text{O}_3$	x_2 [mol %] $\text{Fe}_2^{2+}\text{O}_3$
1	8	0.7	0.3
3	22.85	1.8	1.2
5	37.11	2.5	2.5
10	72.25	4.4	5.6
20	142.85	8.2	11.8
30	213.67	12	18
40	283.29	15.6	24.4

The composition dependence of the molar Curie constant (C_M) is presented in Table 1. For all the glasses experimental values obtained for C_M and consequently for effective magnetic moments (μ_{eff}) are lower than those which correspond to the Fe_2O_3 content, considering that all iron ions are in Fe^{3+} valence state, but they are higher than

those calculated for the case when all iron ions would be Fe^{2+} species (Table 1). Therefore we consider that in these glasses are present both Fe^{3+} and Fe^{2+} ions. The presence of Fe^{3+} and Fe^{2+} ions has been evidenced in other oxide glasses [10,13,21,23,28]. Having in view this supposition and using the atomic magnetic moment values of isolated Fe^{3+} and Fe^{2+} ions: $\mu_{\text{Fe}^{3+}} = 5.92\mu_B$ and $\mu_{\text{Fe}^{2+}} = 4.90\mu_B$ [29], we can estimate in first approximation the molar fraction of these ions in the investigated glasses using the relations:

$$x \cdot \mu_{\text{eff}}^2 = x_1 \cdot \mu_{\text{Fe}^{3+}}^2 + x_2 \cdot \mu_{\text{Fe}^{2+}}^2$$

and

$$x = x_1 + x_2,$$

where $\mu_{\text{eff}} = 2.827\sqrt{C_M/2x}$ are the experimental effective magnetic moment, x_1 and x_2 are the molar fraction of iron ions in Fe^{3+} and Fe^{2+} valence states. The results are presented in Table 1. The content of both Fe^{2+} and Fe^{3+} ions increase with Fe_2O_3 concentration and for $x \geq 10$ mol% the Fe^{2+} molar fraction is higher than that for Fe^{3+} ions. It can be remarked that the obtained data from magnetic susceptibility measurements are in agreement with those obtained from EPR regarding evolution of I and ΔB .

4. Conclusions

Glasses of the system $x\text{Fe}_2\text{O}_3\text{-}(100-x)[3\text{B}_2\text{O}_3\text{-SrO}]$ were obtained over the $0 \leq x \leq 40$ mol % concentration range.

EPR absorption spectra due to Fe^{3+} ions were detected within $0.5 \leq x \leq 40$ mol %. The structure of the spectra and the values of the EPR parameters of resonance lines depend on the Fe_2O_3 concentration. The Fe^{3+} ions in sites of distorted octahedral symmetry subjected to strong crystalline field effects ($g_{\text{eff}} \approx 4.3$) were detected in all studied domain containing Fe_2O_3 ($x \leq 40$ mol %), attesting the structural stability of the vitreous matrix in receiving these ions.

The EPR and magnetic data revealed the presence of Fe^{3+} and Fe^{2+} ions in studied glasses, ions that can be isolated or participates to dipolar and superexchange-type interactions. For samples with $x > 20$ mol % antiferromagnetically coupled iron ions were detected.

Reference

- [1] N. J. Kreidl, J. Non-Cryst. Solids **123**, 337 (1990).
- [2] A. Murali, J. L. Rao, G. L. Narendra, T. Harinathudu, Opt. Mater. **7**, 41 (1997).
- [3] R. P. S. Chakradhar, G. Sivaramaiah, J. L. Rao, N. O. Gopal, Spectrochim. Acta A **62**, 51 (2005).
- [4] D. Loveridge, S. Park, Phys. Chem. Glasses

12, 19 (1971).

[5] A. S. Rao, R. R. Reddy, T. V. R. Rao, J. L. Rao, *Solid State Commun.* **96**, 701 (1995).

[6] L. D. Bogomolova, N. A. Krasilnikova, V. L. Bogdanov, V. D. Khalilev, V. V. Mitrofanov, *J. Non-Cryst. Solids* **188**, 130 (1995).

[7] J. L. Rao, A. Muraly, E. D. Rao, *J. Non-Cryst. Solids* **202**, 215 (1996).

[8] J. Kliava, R. Berger, Y. Servant, J. Emery, J. M. Greneche, J. Trokss, *J. Non-Cryst. Solids* **202**, 205 (1996).

[9] I. Ardelean, M. Peteau, S. Filip, V. Simon, G. Gyorffy, *Solid State Commun.* **102**, 341 (1997).

[10] I. Ardelean, H. H. Qiu, H. Sakata, *Mat. Lett.* **32**, 335 (1997).

[11] R. P. S. Chakradhar, A. Murali, J. L. Rao, *Optical Mat.* **10**, 109 (1998).

[12] D. Boudlich, E. M. Yahiaoui, M. E. Archidi, M. Haddad, A. Nadiri, R. Berger, *Ann. Chim. Sci. Mat.* **23**, 113 (1998).

[13] I. Ardelean, M. Peteau, V. Simon, S. Filip, F. Ciocas, I. Todor, *J. Magn. Magn. Mat.* **196&197**, 257 (1999).

[14] H. B. Pascoal, W. M. Pontuschka, H. Rechenberg, *Appl. Phys.* **A70**, 211 (2000).

[15] S. P. Chaudhuri, S. K. Patra, *J. Mat. Sci.* **35**, 4735 (2000).

[16] J. Dumas, J. L. Tholence, M. Continentino, J. C. Fernandes, R. B. Guimaraes, *J. Magn. Magn. Mat.* **226{230}**, 468 (2001).

[17] C. Prakash, S. Husain, R. J. Singh, S. Mollah, *J. Alloys Compon.* **326**, 47 (2001).

[18] I. Ardelean, P. Pascuta, *Int. J. Mod. Phys.* **B17**, 3889 (2003).

[19] L. K. Wilson, E. J. Friebele, D. L. Kinser, *Proc. Int. Symp. On Amorphous Magnetism*, (Plenum Press, New York, 1975)

[20] I. Ardelean, G. Salvan, M. Peteau, V. Simon, C. Hincinschi, F. Ciocas, *Mod. Phys. Lett.* **B13**, 801 (1999).

[21] B. Kumar, C. H. Chen, *J. Appl. Phys.* **75**, 6760 (1994).

[22] L. K. Wilson, E. J. Friebele, D. L. Kinser, *Proc. Int. Symp. on Amorphous Magnetism* (Plenum Press, New York, 1975).

[23] I. Ardelean, Gh. Ilonca, O. Cozari, V. Simon, S. Filip, *Mater. Lett.* **21**, 321 (1994).

[24] A. Mekki, Kh. A. Ziq, *J. Magn. Magn. Mat.* **189**, 207 (1998).

[25] A. Mekki, D. Holland, Kh. A. Ziq, C. F. McConviele, *J. Non-Cryst. Solids* **272**, 179 (2000).

[26] E. Burzo, I. Ardelean, I. Ursu, *J. Mater. Sci.* **15**, 581 (1980).

[27] E. Burzo, I. Ursu, D. Ungur, I. Ardelean, *Mater. Res. Bull.* **15**, 1273 (1980).

[28] B. Kumar, C. H. Chen, S. Liu, *Phys. Chem. Glasses* **38**, 45 (1992).

[29] L. M. Mulay, *Magnetic Susceptibility* (Interscience, New York, 1973).

*Corresponding author: arde@phys-ubbcluj.ro